ISBN: 978-3-95450-262-2 ISSN: 2673-5350 doi: 10.18429/JACoW-IBIC2025-WEPMO05

TESTING OF SiC BLADE X-RAY BEAM POSITION MONITORS FOR SYNCHROTRON FRONT-ENDS

C. Houghton *, L. Bobb, Diamond Light Source, Oxfordshire, UK

Abstract

X-ray beam position monitors (XBPMs) play a crucial role in accurately measuring the position of the white beam in synchrotron front ends. Traditional XBPM designs typically feature four tungsten blades arranged at the full width at half maximum (FWHM) of the white beam. However, the high absorption and lower thermal resistance of tungsten limit the proximity of the blades to the X-ray source, which may negatively impact measurement precision. This study investigates the performance of an innovative XBPM design that utilises silicon carbide (SiC) blades, which provide enhanced thermal stability and reduced absorption of bending magnet radiation. This advancement may allow for closer placement of the blades to the beam, potentially improving measurement accuracy. This experimental setup aims to assess the impact of SiC blades on measurement accuracy, signal-to-noise ratio, and linearity compared to conventional tungsten XBPMs. The results will offer valuable insights into the benefits and limitations of SiC-based XBPMs compared to their tungsten counterparts.

INTRODUCTION

Diamond is upgrading its front-end tungsten vane XBPMs [1, 2] to handle the higher brilliance and power anticipated for Diamond-II [3]. This provided an opportunity to evaluate a prototype silicon-carbide XBPM as a potential alternative. SiC blades are understood to offer several potential advantages over traditional materials, such as reduced absorption of bending-magnet background radiation and improved thermal stability of the signal. Monochromatic XBPMs utilising SiC have previously been successfully benchmarked against conventional single-crystal diamond XBPMs [4], demonstrating comparable performance under operating conditions.

For simplicity and consistency, the prototype was installed using the existing blade holder design, see Fig. 1. Each beamline front-end contains two XBPMs spaced approximately 4 m apart, enabling angular measurements of the photon beam. In this study, the prototype SiC vane XBPM [5] replaced the downstream XBPM-02 located 16.53 m from the insertion device sourcepoint. The upstream XBPM-01 is a tungsten vane XBPM installed in 2007 at a distance of 12.25 m from the sourcepoint. Simultaneous measurements from both devices allowed for direct comparison.

The SiC blades used in this prototype consist of doped epitaxial layers forming a p-n junction: a 15 µm thick n- nitrogen-doped inactive layer and a 1.5 µm thick p+ phosphorous-doped active layer grown on an n+ substrate, see Fig. 2. At the chips edge the p+ layer is selectively removed, creating an inactive border region, this will act as a photon filter limiting low photon energy (UV and soft X-rays) contributions [6]. The blades are mounted between a cathode and an anode, allowing for bias application and photo-current measurement. Unless stated otherwise throughout this experiment, a bias of −20 V was applied to the anode of each SiC blade.

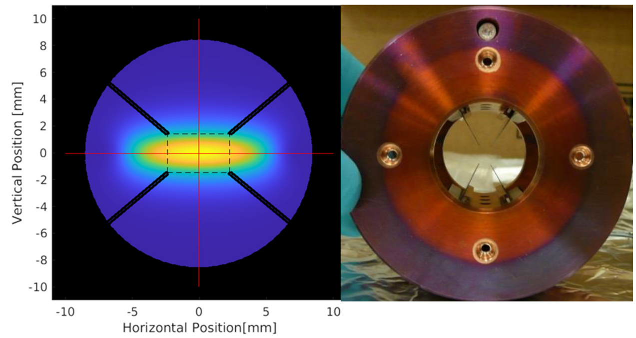

Figure 1: Left: Schematic of a vane XBPM, showing the blades interacting with the photon beam. Right: Image of a tungsten vane XBPM.

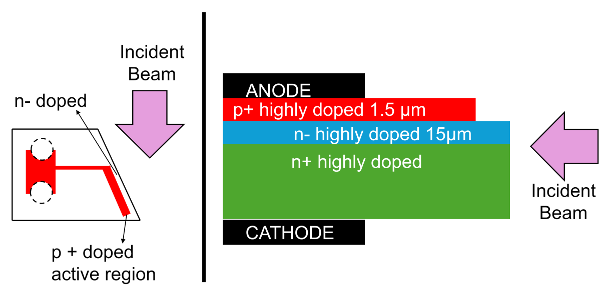

Figure 2: Diagram of the SiC blade setup. Left: top view focusing on the active SiC area with a built-in photon filter to reduce UV light. Right: side view showing doped SiC layers, the anode and cathode [6].

ELECTRICAL TESTING

Without beam incident to the XBPM a ±10 V input voltage was sequentially applied to the anode of each blade. The current response was measured of the input blade and the voltage output of the remaining three blades was recorded, see Fig. 3. The results for the tungsten vane XBPM demonstrated an output current within µA range and showed no significant response to the applied voltage, indicating effective electrical isolation between the blades. Conversely, the silicon carbide vane XBPM saw a markedly higher current output, reaching the mA range, along with a significant positive correlation to the input voltage. Notably, the application

* claire.houghton@diamond.ac.uk

© Content from this work may be used under the terms of the CC BY 4.0 licence (© 2024). Any distribution of this work must maintain attribution to the author(s), title of the work, publisher, and DOI.

ISBN: 978-3-95450-262-2 ISSN: 2673-5350 doi: 10.18429/JACoW-IBIC2025-WEPMO05

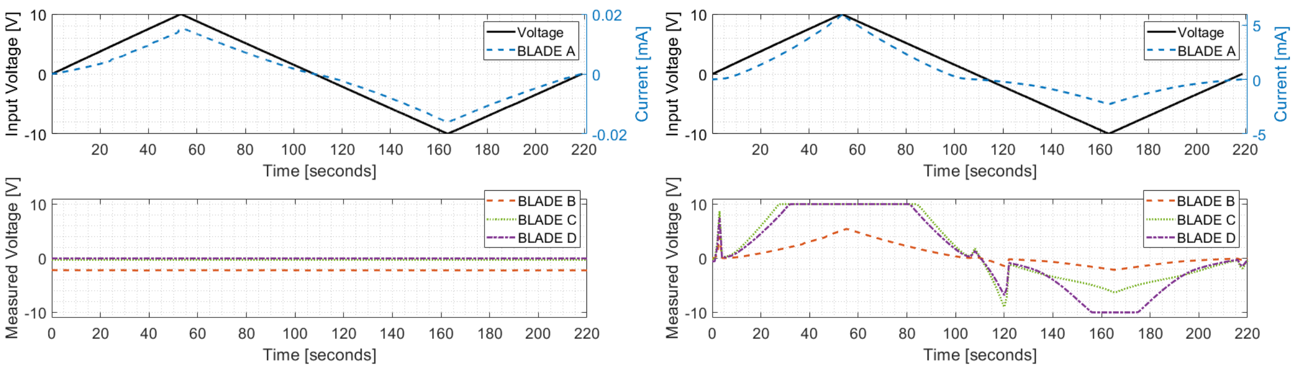

Figure 3: Graphs showing the results of electrical testing of the front-end XBPMs without beam. Top: shows the input voltage applied and measured current for a given blade. Bottom: The voltage response of the remaining three blades. Left: Tungsten vane XBPM, input voltage applied to blade A. Right: SiC vane XBPM, input voltage applied to blade A.

of voltage to blade A in the SiC configuration consistently resulted in saturation of the output electronics for blade D at ±10 V, which suggests electrical crosstalk within the device. There are also artefacts as the input voltage crosses 0 V, causing a spike in the measured voltages, which are not consistent in amplitude for each zero point. Focusing on the negative voltage region, as this is the direction the bias is applied in operation, the response for blade B is minimal compared to the other blades, suggesting the electrical issues are not consistent across the whole device.

BEAM POSITION MEASUREMENT

To further characterise device performance, offsets were applied to nearby Electron Beam Position Monitors (EBPMs) to raster the X-ray beam across the XBPMs, with the resulting Δ/Σ response curves presented in Fig. 4. The tungsten vane XBPM produced the expected square response profile, with some axis coupling, which is likely due to degradation of the ceramic insulators [7]. In contrast, the SiC XBPM exhibited substantial and unexpected axis coupling, consistent with the electrical tests indicating significant crosstalk between quadrants.

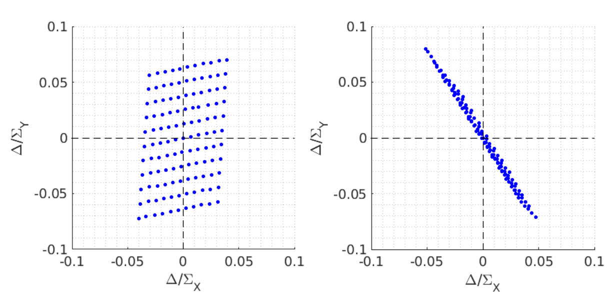

Figure 4: Scatter plot of XBPM response during a 2D raster scan, with each point representing an EBPM move of ±0.01 mm. Left: Tungsten vane XBPM. Right: SiC vane XBPM

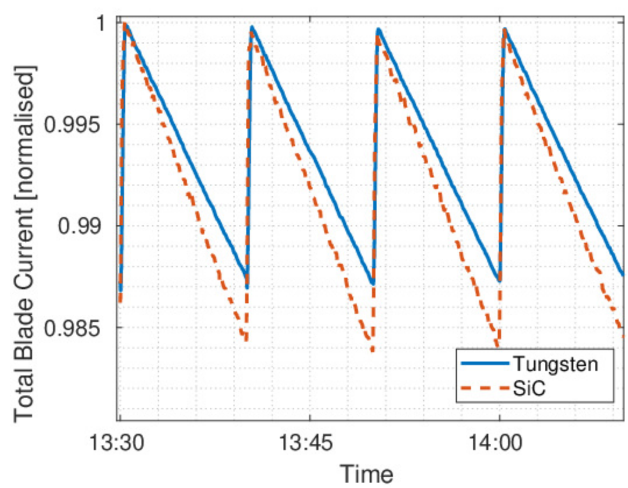

Figure 5: Normalised total blade current for tungsten and SiC XBPMs across several 10-minute top-up cycles.

BEAM CURRENT MEASUREMENT

Figure 5 shows the normalised total blade current for both tungsten and SiC XBPMs during several 10-minute top-up cycles. The total current of the prototype SiC blades mirrored the decay trend observed in the tungsten XBPM, highlighting the consistency between the two detection methods.

Among the four blades monitored, blade B saw a current spike during each top-up, as shown in Fig. 6, a behaviour not observed in the other blades. This does not necessarily indicate a fault as similar artefacts are observed on some tungsten vane XBPMs during top-up. After isolating and removing the data corresponding to these spikes in blade B, all SiC blades experienced an approximately 1% decline in current during the intervals between injections.

In response to these findings, the external grounding of the XBPM was adjusted to secure a robust cathode connection. After this intervention, as seen in Fig. 7, blade B continued to display its previous decay and top-up characteristics, while blades A, C, and D no longer saw top-up. This aligns

Content from this work may be used under the terms of the CC BY 4.0 licence (© 2024). Any distribution of this work must maintain attribution to the author(s), title of the work, publisher, and DOI.

ISBN: 978-3-95450-262-2 ISSN: 2673-5350 doi: 10.18429/JACoW-IBIC2025-WEPMO05

Content from this work may be used under the terms of the CC BY 4.0 licence (© 2024). Any distribution of this work must maintain attribution to the author(s), title of the work, publisher, and DOI.

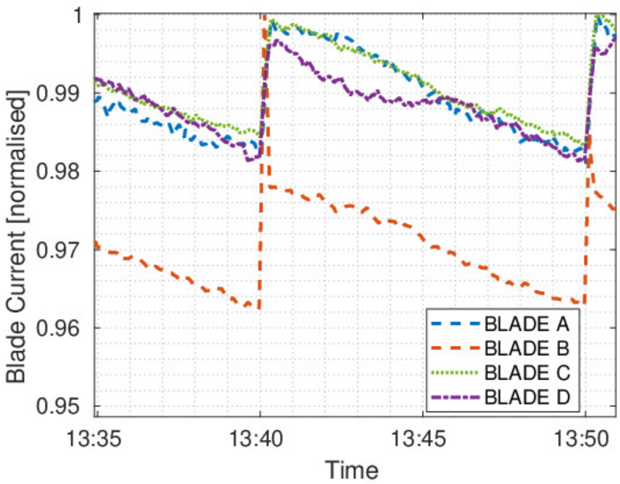

Figure 6: Normalised individual blade currents of the SiC XBPM across several 10-minute top-up cycles.

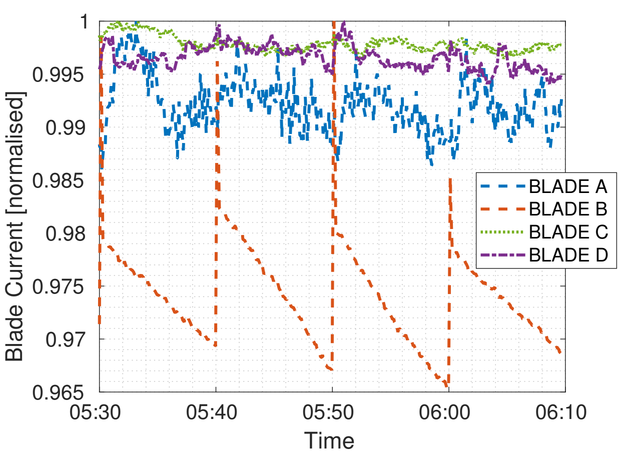

Figure 7: Normalised individual blade currents for the SiC XBPM across several 10-minute top-up cycles, with robust cathode grounding.

with the electrical testing results, indicating that blade B has the best electrical isolation of the SiC blades. The remaining blades appear to have a short. When the grounding connection is improved, this creates a faster electrical path that bypasses the diode blades, leading to reduced current response measured on the blades.

CONCLUSION

A prototype SiC vane XBPM was tested in a synchrotron beamline front-end to evaluate its potential as an alternative to traditional tungsten vane XBPMs. Beam position measurements revealed unexpected axis coupling, limiting its effectiveness as a position monitor in its current form. Electrical testing indicated significant crosstalk between blades, with blade B exhibiting behaviour closest to the expected response. Despite these challenges, the SiC XBPM successfully tracked beam current decay similarly to the tungsten vane XBPM, with blade B showing distinct current spikes during top-up injections. The study highlights the potential of SiC blades in XBPMs while acknowledging the need for further research to address the identified challenges.

FUTURE WORK

Following this initial evaluation of the prototype SiC vane XBPM, several next steps are planned to address the observed electrical isolation issues. This could be caused by the anode and cathode extending slightly beyond the size of the blade, resulting in no material between these plates. Due to the relative softness of SiC, the mechanical pressure from the mounting screws and the thermal expansion of the blades in the beam have likely reduced the separation between these plates, potentially causing them to touch, see Fig. 8. This would explain the electrical issues we have observed.

To address this, the prototype SiC vane XBPM will be removed and returned to the manufacturer [5,8], where work will be conducted to improve the electrical isolation. This evaluation has highlighted that while the usage of SiC blades is similar to tungsten, the diode nature of the blades requires more consideration on how to ensure robust electrical isolation through shipping and heating due to the beam. The current response observed shows promise that with some changes to the mounting of the blade, SiC can be used as an alternative to tungsten in white-beam X-ray Beam Position Monitors.

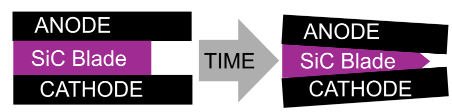

Figure 8: Diagram showing the theorised cause of the electrical issues, with the anode and cathode extending past the SiC blade.

ACKNOWLEDGEMENTS

The authors would like to thank the I22 beamline team for providing access to the front-end for this experiment. We are grateful to Samuel Jackson, Diamond Light Source, for his assistance with data collection and electrical testing. Our thanks also go to FMB Berlin GmbH for manufacturing the XBPM assembly, and to SenSiC GmbH for producing the prototype SiC blade.

REFERENCES

[1] P. Mortazavi *et al.*, "High Flux Photon Beam Monitor", *Nucl. Instrum. Methods Phys. Res. A*, vol. 246, pp. 389-393, 1986. `doi:10.1016/0168-9002(86)90115-4`

[2] T. Warwick *et al.*, "Prototype photon position monitors for undulator beams at the Advanced Light Source", *Rev. Sci. Instrum.*, vol. 63, pp. 550-553, 1992. `doi:10.1063/1.1142703`

[3] R. P. Walker *et al.*, *Diamond-II Technical Design Report*, Diamond Light Source Ltd., Oxfordshire, UK, Tech.

ISBN: 978-3-95450-262-2 ISSN: 2673-5350 doi: 10.18429/JACoW-IBIC2025-WEPMO05

Rep., 2022, https://www.diamond.ac.uk/Home/News/LatestNews/2022/14-10-22.html

[4] C. Houghton, C. Bloomer, L. Bobb, "A direct experimental comparison of single-crystal CVD diamond and silicon carbide X-ray beam position monitors", *J Synchrotron Radiat.*, vol. 30, no. 5, pp. 876-884, 2023. doi:10.1107/S1600577523005623

[5] SenSiC GmbH, https://www.sensic.ch/

[6] M. Camarda, private communication.

[7] C. Bloomer and G. Rehm, "Operation of Diamond Light Source XBPMs with Zero Bias", in *Proc. IBIC'13*, Oxford, UK, Sep. 2013, paper TUPC10, pp. 376–379.

[8] FMB Berlin, https://www.fmb-berlin.de/index.php/en/

© Content from this work may be used under the terms of the CC BY 4.0 licence (© 2024). Any distribution of this work must maintain attribution to the author(s), title of the work, publisher, and DOI.